Methylene-Bridged Heterobinuclear Complexes of Iridium and Ruthenium: Models for Bimetallic Fischer−Tropsch Catalysts

Maria Michela Dell'Anna,† Steven J. Trepanier, Robert McDonald,‡ and Martin Cowie*

Chemistry Department, University of Alberta, Edmonton, Alberta, Canada T6G 2G2

Received July 25, 2000

The heterobinuclear complexes $[IrRu(CO)_3(\mu\text{-}H)(dppm)_2]$ (**1**) and $[IrRuH(CO)_3(\mu\text{-}CO)(dppm)_2]$ (**2**) are prepared from the reactions of $[PPN][HRu(CO)_4]$ with $[IrCl(dppm)_2]$ and $[Ir(CO)(dppm)_2][Cl]$, respectively (PPN = $(Ph_3P)_2N$; dppm = $Ph_2PCH_2PPh_2$). Protonation of both monohydride species yields the dihydride $[IrRu(CO)_3(\mu\text{-}H)_2(dppm)_2][BF_4]$ (**3**), which under an atmosphere of carbon monoxide gives $[IrRu(CO)_4(dppm)_2][BF_4]$ (**4**). The methylene-bridged complex $[IrRu(CO)_3(\mu\text{-}CH_2)(\mu\text{-}CO)(dppm)_2][BF_4]$ (**5**) is obtained by the reaction of compound **4** with diazomethane at ambient temperature. Although **5** does not react further with diazomethane under these conditions, carbonyl abstraction using trimethylamine oxide in the presence of CH_2N_2 yields the methylene-bridged ethylene adduct $[IrRu(C_2H_4)(CO)_3(\mu\text{-}CH_2)(dppm)_2][BF_4]$ (**6**). Labeling studies indicate that the majority of the ^{13}C-labeled methylene group of **5** remains in the bridging site, with approximately 10% of the label incorporated into the ethylene formed. Compound **6** can also be prepared from **5** and ethylene in the presence of Me_3NO. The compounds $[IrRuL(CO)_3(\mu\text{-}CH_2)(dppm)_2][BF_4]$ (L = NCMe, PMe_3, CH_2CHCN) can also be prepared from **5** in the presence of Me_3NO or by ethylene displacement from **6**. Although the PMe_3 adduct has this group bound to Ir, as for the ethylene ligand in **6**, the acrylonitrile and acetonitrile groups are bound to Ru. Furthermore, the acrylonitrile ligand is N-bound through the cyano group, analogous to the acetonitrile ligand. The structures of $[IrRuH(CO)_3(\mu\text{-}CO)(dppm)_2]$ (**2**), $[IrRu(CO)_3(\mu\text{-}CH_2)(\mu\text{-}CO)(dppm)_2][BF_4]$ (**5**), and $[IrRu(PMe_3)(CO)_3(\mu\text{-}CH_2)(dppm)_2][BF_4]$ (**7**) have been determined by X-ray methods. Compounds **2** and **7** have comparable edge-shared bioctahedral structures in which the geometries at the different metals in each structure are similar. The bridging carbonyl in **2** is replaced by a methylene group in **7**, and the Ir-bound hydride is replaced by PMe_3. Compound **5** has bridging CO and CH_2 groups on opposite faces of the $IrRuP_4$ framework with two terminal carbonyls on Ru and one on Ir.

Introduction

The Fischer−Tropsch (FT) process, in which synthesis gas ($CO + H_2$) is converted into a variety of hydrocarbons, utilizes group 8 or 9 metals as catalysts.[1] Although all of the metals in these groups are active, only Co and Fe are widely used commercially. Ruthenium is actually the most active catalyst,[2] but its greater expense limits its commercial utility. A comparison of these catalysts shows that the different metals give rise to substantially different product distributions.[3,4] For example, iron yields mainly linear alkenes and oxygenates, cobalt gives mostly linear alkanes, and ruthenium gives high molecular-weight hydrocarbons, while rhodium yields oxygenates and hydrocarbons.

Reports of improved product selectivity in processes such as alkane isomerization and hydrogenolysis, when bimetallic catalysts were used instead of monometallic catalysts,[5] suggested to us that a similar approach might also be promising in FT chemistry. A few reports have already appeared on the use of mixed RuCo catalysts in FT chemistry, in which improved selectivity and activity were observed compared to the Co-supported catalysts alone.[6,7] In addition, improved activities and selectivities have been noted using combined group 8/9 bimetallic catalysts in the formation of oxygenates from syngas[8] or in ethylene hydroformylation.[9]

* To whom correspondence should be addressed. McCalla Research Professor, 1999−2000. Fax: (780) 492-8231. E-mail: martin.cowie@ualberta.ca.

† Present address: Instituto di Chimica, Politechnico di Bari, Bari, Italy.

‡ X-ray Crystallography Laboratory.

(1) (a) Biloen, P.; Sachtler, W. M. H. *Adv. Catal.* **1981**, *30*, 165. (b) Van der Laan, G. P.; Beenackers, A. A. C. M. *Catal. Rev.-Sci. Eng.* **1999**, *41*, 255. (c) Schulz, H. *Appl. Catal. A* **1999**, *186*, 3.

(2) Vannice, M. A. *J. Catal.* **1975**, *37*, 462.

(3) Vannice, M. A. *J. Catal.* **1975**, *37*, 449.

(4) (a) Bhasin, M.; Hartley, W. J.; Ellgen, P. C.; Wilson, T. P. *J. Catal.* **1978**, *54*, 120. (b) Ichikawa, M. *Bull. Chem. Soc. Jpn.* **1978**, *51*, 2273. (c) Ichikawa, M. *J. Catal.* **1979**, *56*, 127. (d) Watson, P. R.; Somorjai, G. A. *J. Catal.* **1981**, *72*, 347. (e) Watson, P. R.; Somorjai, G. A. *J. Catal.* **1982**, *74*, 282. (f) Kip, B. J.; Hermans, E. G. F.; van Wolput, J. H. M. C.; Haermans, N. M. A.; van Grondelle, J.; Prins, R. *Appl. Catal.* **1987**, *35*, 109. (g) Lavalley, J. C.; Saussey, J.; Lamotte, J.; Breault, R.; Hindermann, J. P.; Kiennemann, A. *J. Phys. Chem.* **1990**, *94*, 5941. (h) Bowker, M. *Catal. Today* **1992**, *15*, 77.

(5) Sinfelt, J. H. *Bimetallic Catalysts: Discoveries, Concepts, and Applications*; Wiley: New York, 1983; Chapter 2.

(6) Iglesia, E.; Soled, S. L.; Fiato, R. A.; Via, G. H. *J. Catal.* **1993**, *143*, 345.

10.1021/om000639b CCC: $20.00
Publication on Web 12/02/2000

Our interest in using heterobinuclear complexes of the group 8 and 9 metals as models for bimetallic catalysts[10−13] led us to question whether combinations of these metals could lead to unusual examples of C−C bond formation of relevance to FT chemistry. In particular, we were interested in determining the functions of the different metals in such processes. In an earlier study[13] we observed that a RhOs complex promoted facile coupling of diazomethane-generated methylene groups, yielding either the allyl−methyl complex [RhOs(η^1-C_3H_5)(CH_3)($CO)_3$(dppm)$_2$][BF_4] (dppm = $Ph_2PCH_2PPh_2$) or a butanediyl-containing product, [RhOs(C_4H_8)($CO)_3$(dppm)$_2$][BF_4], depending upon the temperature of the reaction. Labeling studies allowed us to suggest a mechanism, and a proposal was put forward rationalizing the functions of the different metals in these unusual transformations. An obvious extension of this study was to investigate other group 8/9 metal combinations for a comparison to the RhOs chemistry, and herein we present our initial findings on the related IrRu chemistry.

Experimental Section

General Comments. All solvents were dried (using appropriate drying agents), distilled before use, and stored under nitrogen. Reactions were performed under an argon atmosphere using standard Schlenk techniques. Ammonium hexachloroiridate(IV) was purchased from Vancouver Island Precious Metals, and ruthenium trichloride hydrate was obtained from Colonial Metals Inc. Carbon-13-enriched CO (99.4% enrichment) was purchased from Isotec Inc. Diazomethane was generated from Diazald, which was purchased from Aldrich. The compounds $Ru_3(CO)_{12}$,[14] [PPN][$HRu(CO)_4$] (PPN = $(Ph_3P)_2N$)),[15] [IrCl(dppm)$_2$],[16] and [Ir(CO)(dppm)$_2$][Cl][17] were prepared by the published procedures.

NMR spectra were recorded on a Bruker AM-400 spectrometer operating at 400.1 MHz for ^{1}H, 161.9 MHz for ^{31}P, and 100.6 MHz for ^{13}C nuclei. The $^{13}C\{^1H\}\{^{31}P\}$ NMR spectra were obtained on a Bruker WH-200 spectrometer operating at 50.3 MHz. Infrared spectra were obtained on a Nicolet Magna 750 FTIR spectrometer with a NIC-Plan IR microscope. The elemental analyses were performed by the microanalytical service within the department. In cases where the analyses deviated significantly from the calculated values, the samples were also analyzed by Canadian Microanalytical Service Ltd. using V_2O_5, PbO_2, and Sn combustion catalysts. The values for the C analyses remained low, presumably due to the formation of metal carbides. Electron ionization mass spectra were run on a Micromass ZabSpec. In all cases the distribution of isotope peaks for the appropriate parent ion matched very closely that calculated for the formulation given.

Preparation of Compounds. Spectroscopic data for the compounds prepared are presented in Table 1.

(a) [IrRu(CO)$_3$(μ-H)(dppm)$_2$] (1). The compound [PPN][$HRu(CO)_4$] (0.040 g, 0.06 mmol) was added to [IrCl(dppm)$_2$] (0.054 g, 0.06 mmol) dissolved in 5.0 mL of THF. The solution immediately turned green, and a white precipitate formed (PPNCl). The green solution was concentrated under vacuum to ca. 2 mL and the solution allowed to slowly evaporate under an argon atmosphere. A green precipitate formed. Compound **1** is extremely air sensitive; therefore, all attempts to obtain elemental analyses resulted in sample decomposition. Characterization was based on spectral methods, on the conversion of **1** to **2** by addition of carbon monoxide, and by the reverse transformation upon reaction of **2** with Me_3NO.

(b) [IrRu(H)(CO)$_3$(μ-CO)(dppm)$_2$] (2). The compound [Ir(CO)(dppm)$_2$][Cl] (1.026 g, 1.00 mmol) was suspended in 30 mL of THF, to which a suspension of [PPN][$HRu(CO)_4$] (0.753 g, 1.00 mmol) in 30 mL of THF was added by cannula. This mixture was stirred for 12 h, resulting in an orange-brown solution and a white precipitate of [PPN][Cl]. The solution was concentrated under vacuum to ca. 10 mL, and 30 mL of ether was added to precipitate a yellow solid. The solid was recrystallized from benzene/ether and dried in vacuo (68% yield). Anal. Calcd for $C_{72}H_{63}O_4P_4IrRu$: C, 61.36; H, 4.51. Found: C, 61.79; H, 4.79. This compound was found to have three molecules of benzene per complex molecule after drying in vacuo.

(c) [IrRu(CO)$_3$(μ-H)$_2$(dppm)$_2$][BF_4] (3). Method i. Compound **1** (50 mg, 0.044 mmol) was dissolved in 5 mL of THF, and HBF_4·OMe_2 (6 μL, 0.049 mmol) was added, causing the solution to change from green to orange with the formation of a yellow precipitate. This precipitate was separated by filtration and washed with three 5 mL portions of diethyl ether (yield 74%). Anal. Calcd for $C_{53}H_{46}BF_4O_3P_4IrRu$: C, 51.55; H, 3.75. Found: C, 51.01; H, 3.65.

Method ii. Compound **2** (300 mg, 0.255 mol) was dissolved in 15 mL of THF, and HBF_4·$O(CH_3)_2$ (31 μL, 0.255 mmol) was added, causing the solution to change immediately to orange. After 30 min a yellow precipitate formed. Ether (40 mL) was then added to precipitate the remaining solid. The solid obtained by this route was found to be a 1:1 mixture of **3** and **4**.

(d) [IrRu(CO)$_4$(dppm)$_2$][BF_4] (4). Compound **3** from method i of part c or the mixture of solids from preparation ii of part c was suspended in 20 mL of CH_2Cl_2 and stirred under a CO atmosphere for several hours, after which time a yellow slurry remained. Ether (40 mL) was then added to precipitate the remaining solid, which was then recrystallized from CH_2Cl_2/ether and dried in vacuo (82% yield based upon **1** or **2**). Anal. Calcd for $C_{54}H_{44}BF_4O_4P_4IrRu$: C, 51.44; H, 3.52. Found: C, 50.96; H, 3.65. MS *m*/*z* 1175 ($M^+ - BF_4$).

(e) [IrRu(CO)$_4$(μ-CH$_2$)(dppm)$_2$][BF_4] (5). Compound **4** (100 mg, 0.079 mmol) was suspended in 15 mL of CH_2Cl_2. Diazomethane, generated from 300 mg of Diazald, was bubbled through this solution for 30 min, after which the reaction mixture became clear yellow. The solvent was evaporated to 5 mL under an argon stream, and 30 mL of ether was added to precipitate a bright yellow solid. The solid was then recrystallized from CH_2Cl_2/ether and dried in vacuo (92% yield). Anal. Calcd for $C_{55}H_{46}BF_4O_4RuP_4Ir$: C, 51.81; H, 3.64. Found: C, 51.37; H, 3.84%. MS *m*/*z* 1189 ($M^+ - BF_4$).

(f) [IrRu(C_2H_4)(CO)$_3$(μ-CH$_2$)(dppm)$_2$][BF_4] (6). Method i. Compound **5** (10 mg, 0.0078 mmol) and Me_3NO (0.60 mg, 0.0078 mmol) were placed in an NMR tube containing an

(7) (a) Beuther, H.; Kobylinski, T. P.; Kibby, C. L.; Pannell, R. B. U.S. Patent 4,585,798, 1986; assigned to Gulf Research and Development Co. (b) Beuther, H.; Kibby, C. L.; Kobylinski, T. P.; Pannell, R. B. U.S. Patent 4,413,064, 1983; assigned to Gulf Research and Development Co. (c) Beuther, R. B.; Kibby, C. L.; Kobylinski, T. P.; Pannell, R. B. U.S. Patent 4,493,905, 1985; assigned to Gulf Research and Development Co. (d) Kobylinski, T. P.; Kibby, C. L.; Pannell, R. B.; Eddy, E. L. U.S. Patent 4,605,676, 1986; assigned to Chevron Research Co.

(8) See for example: (a) Fukushima, T.; Arakawa, H.; Ichikawa, M. *J. Phys. Chem.* **1985**, *89*, 4440. (b) Ichikawa, M. *Polyhedron* **1988**, *7*, 2351. (c) Xiao, F.-S.; Fukuoka, A.; Ichikawa, M. *J. Catal.* **1992**, *138*, 206.

(9) Xiao, F.-S.; Ichikawa, M. *J. Catal.* **1994**, *147*, 578.

(10) Hilts, R. W.; Franchuk, R. A.; Cowie, M. *Organometallics* **1991**, *10*, 304.

(11) Sterenberg, B. T.; Hilts, R. W.; Moro, G.; McDonald, R.; Cowie, M. *J. Am. Chem. Soc.* **1995**, *117*, 245.

(12) Sterenberg, B. T.; McDonald, R.; Cowie, M. *Organometallics* **1997**, *16*, 2297.

(13) Trepanier, S. J.; Sterenberg, B. T.; McDonald, R.; Cowie, M. *J. Am. Chem. Soc.* **1999**, *121*, 2613.

(14) Bruce, M. I.; Matisons, J. G.; Wallis, R. C.; Patrick, J. M.; Skelton, B. W.; White, A. H. *J. Chem. Soc., Dalton Trans.* **1983**, 2365.

(15) Walker, H. W.; Ford, P. C. *J. Organomet. Chem.* **1981**, *214*, C43.

(16) Hilts, R. W.; Franchuk, R. A.; Cowie, M. *Organometallics* **1991**, *10*, 1297.

(17) Miller, J. S.; Caulton, K. G. *J. Am. Chem. Soc.* **1975**, *97*, 1067.

Table 1. Spectroscopic Data for the Compounds

compd	IR[a,b]	NMR[c,d] $\delta(^{31}P\{^1H\})$[e]	NMR[c,d] $\delta(^1H)$[f,g]	NMR[c,d] $\delta(^{13}C\{^1H\})$[g]
$[IrRuH(CO)_3(dppm)_2]$ (**1**)	1926 (s), 1835 (m)	48.4 (m), 15.0 (m)[h]	−9.06 (tt, $^2J_{PH}$ = 12,12 Hz, 1H), 3.87 (m, 4H),[h,i] −9.11 (tt, $^2J_{PH}$ = 12, 12 Hz, 1H), 4.13 (m, 2H), 3.75 (m, 2H)[h,j]	215.8 (br, 2C), 185.6 (t, $^2J_{PC}$ = 14 Hz, 1C),[h,i] 187.4 (br, 1C), 212.0 (br, 1C), 223.5 (br, 1C)[h,j]
$[IrRuH(CO)_4(dppm)_2]$ (**2**)	1953 (s), 1897 (s), 1857 (s), 1685 (m)	40.3 (m), 1.8 (m)[h]	5.85 (m, 2H), 3.18 (m, 2H), −9.95 (t, $^2J_{PH}$ = 10 Hz, 1H)[h]	262.7 (m), 218.2 (m), 207.8 (t, $^2J_{PC}$ = 16.0 Hz), 189.1 (m)[h,k]
$[IrRu(CO)_3(\mu\text{-}H)_2(dppm)_2][BF_4]$ (**3**)	2050 (s), 2032 (s), 1963 (m)	34.6 (m), 13.0 (m)	4.14 (m, 4H), −8.87 (tt, $^2J_{PH}$ = 13, 7 Hz, 2H)	198.3 (t, $^2J_{PC}$ = 11 Hz, 2C), 175.5 (t, $^2J_{PC}$ = 15 Hz, 1C)
$[IrRu(CO)_4(dppm)_2][BF_4]$ (**4**)	1983 (s), 1962 (s)	30.0 (m), −10.0 (m)	4.30 (m, 4H)	206.7 (t, $^2J_{PC}$ = 13 Hz, 2C), 197.3 (t, $^2J_{PC}$ = 15 Hz, 1C), 172.2 (t, $^2J_{PC}$ = 10 Hz, 1C)
$[IrRu(CO)_4(\mu\text{-}CH_2)(dppm)_2][BF_4]$ (**5**)	2039 (m), 1965 (s), 1783 (m)	30.2 (m), 3.1 (m)	3.87 (m, 2H), 3.57 (tt, $^3J_{PH}$ = 23, 11 Hz, 2H), 3.08 (m, 2H)	211.3 (dm, $^2J_{CC}$ = 23 Hz, 1C), 196.0 (t, $^2J_{PC}$ = 11 Hz, 1C), 191.7 (dt, $^2J_{PC}$ = 12 Hz, $^2J_{CC}$ = 23 Hz, 1C), 179.0 (t, $^2J_{PC}$ = 11 Hz, 1C)
$[IrRu(C_2H_4)(CO)_3(\mu\text{-}CH_2)(dppm)_2][BF_4]$ (**6**)	1962 (s), 2021 (s)	23.1 (m), −5.3 (m)	6.20 (tt, $^3J_{PH}$ = 10, 8 Hz, 2H), 4.46 (m, 2H), 3.28 (m, 2H), 1.73 (br, 2H), 0.54 (br, 2H)[j]	200.1 (t, $^2J_{PC}$ = 15 Hz, 1C), 195.8 (t, $^2J_{PC}$ = 11 Hz, 1C), 191.9 (t, $^2J_{PC}$ = 6 Hz, 1C), 64.3 (s, 1C), 22.6 (s), 26.4 (s)
$[IrRu(PMe_3)(CO)_3(\mu\text{-}CH_2)(dppm)_2][BF_4]$ (**7**)	2057 (w), 1985 (s), 1950 (s), 1921 (s)	24.8 (m), −12.7 (m), −59.1 (tt, $^2J_{PP}$ = 10, 9 Hz)	4.86 (m, 2H), 4.17 (ttd, $^3J_{PH}$ = 11, 7, 7 Hz, 2H), 3.44 (m, 2H), 0.95 (d, $^2J_{PH}$ = 10 Hz, 9H)	203.9 (t, $^2J_{PC}$ = 7 Hz, 1C), 198.9 (td, $^2J_{PC}$ = 18 Hz, $^3J_{PC}$ = 20 Hz, 1C), 183.3 (td, $^2J_{PC}$ = 15, 4 Hz, 1C)
$[IrRu(NCMe)(CO)_2(\mu\text{-}CH_2)(\mu\text{-}CO)(dppm)_2][BF_4]$ (**8**)	1954 (s), 1933 (s), 1745 (m)	37.9 (m), 6.94 (m)	3.97 (m, 2H), 3.94 (m, 2H), 2.88 (m, 2H), 1.14 (s, 3H)	219.1 (br t, $^2J_{PC}$ = 10 Hz, 1C), 195.6 (t, $^2J_{PC}$ = 12 Hz, 1C), 182.5 (t, $^2J_{PC}$ = 11 Hz, 1C)
$[IrRu(\eta^1\text{-}NC(H)C{=}CH_2)(CO)_3(\mu\text{-}CH_2)(dppm)_2][BF_4]$ (**9**)	1965 (s), 1948 (s), 1755 (m)	37.2 (m), 6.6 (m)	3.91 (m, 2H), 3.96 (m, 2H), 2.89 (m, 2H), 5.18 (d, $^3J_{HH}$ = 18 Hz, 1H), 5.68 (d, $^3J_{HH}$ = 11 Hz, 1H),4.68 (dd, $^3J_{HH}$ = 18, 11 Hz, 1H)	218.8 (t, $^2J_{PC}$ = 10 Hz, 1C), 195.5 (t, $^2J_{PC}$ = 12 Hz, 1C), 182.2 (t, $^2J_{PC}$ = 11 Hz, 1C)

[a] IR abbreviations: s = strong, m = medium, w = weak. [b] Nujol mull or CH_2Cl_2 cast unless otherwise stated; in units of cm^{-1}. [c] NMR abbreviations: s = singlet, m = multiplet, t = triplet, d = doublet, br = broad, tt = triplet of triplets, dt = doublet of triplets, ttd = triplet of triplets of doublets, td = triplet of doublets. [d] NMR data at 25 °C in CD_2Cl_2 unless otherwise stated; in units of ppm. [e] ^{31}P chemical shifts referenced to external 85% H_3PO_4. [f] Chemical shifts for the phenyl hydrogens are not given. [g] ^1H and ^{13}C chemical shifts referenced to TMS. [h] In THF. [i] 25 °C. [j] −80 °C. [k] −60 °C.

ethylene atmosphere. Upon addition of CD_2Cl_2 (0.5 mL), the solution immediately changed to orange and then to yellow within 1 min. Elemental analyses were not performed, due to facile loss of ethylene upon workup.

Method ii. Compound **5** (10 mg, 0.0078 mmol) and Me_3NO (0.6 mg, 0.0078 mmol) were placed in an NMR tube, and CD_2Cl_2 (0.5 mL) was added. The solution was mixed for ca. 20 s, producing an orange-red solution, and then cooled to −78 °C. CH_2N_2 was then bubbled through the cold solution for 1 min, resulting in a yellow solution. ^{31}P and ^1H NMR spectroscopy indicated that the product was compound **6**.

(g) $[IrRu(PMe_3)(CO)_3(\mu\text{-}CH_2)(dppm)_2][BF_4]$ (7). Method i. Compound **5** (40 mg, 0.031 mmol) was dissolved in 2 mL of CH_2Cl_2, and PMe_3 (100 μL of a 1.0 M THF solution, 0.10 mmol) was added. The solution was stirred for 8 h. Ether (20 mL) was then added to precipitate a yellow solid. The solid was recrystallized from CH_2Cl_2/ether and dried in vacuo (48% yield). Anal. Calcd for $C_{57.2}H_{55.4}BCl_{0.4}F_4O_3P_5IrRu$: C, 51.27; H, 4.17; Cl, 1.05. Found: C, 51.12; H, 4.17; Cl, 0.57. MS: *m*/*z* 1237 ($M^+ - BF_4$). The fractional methylene chloride (0.2) of crystallization results because desolvation occurs readily upon removal of the crystals from the mother liquor. However, even storage under vacuum for extended periods does not result in complete solvent loss. The presence of CH_2Cl_2 has been established by analysis for Cl and by ^1H NMR spectroscopy in chloroform.

Method ii. Compound **6** (0.0078 mmol) was prepared in situ in an NMR tube containing 0.5 mL of CD_2Cl_2. One equivalent of PMe_3 (7.8 μL of a 1.0 M THF solution, 0.0078 mmol) was added, and the solution was mixed for 1 min. ^1H and ^{31}P NMR spectroscopy indicated complete conversion to **7**.

(h) $[IrRu(NCCH_3)(CO)_3(\mu\text{-}CH_2)(dppm)_2][BF_4]$ (8). Compound **5** (60.0 mg, 0.047 mmol), trimethylamine oxide (3.5 mg, 0.047 mmol), and acetonitrile (0.10 mL, 1.9 mmol) were placed into a flask, and 3 mL of CH_2Cl_2 was added. The solution immediately turned orange. After the mixture was stirred for 15 min, 20 mL of ether was added, resulting in the precipitation of an orange solid. After it was filtered, this solid was recrystallized from CH_2Cl_2/ether and dried in vacuo (87% yield). Anal. Calcd for $C_{56}H_{49}NBF_4O_3P_4IrRu$: C, 52.22; H, 3.83; N, 1.09. Found: C, 51.52; H, 3.74; N, 1.29. MS: *m*/*z* 1161 ($M^+ - BF_4 - NCCH_3$).

(i) $[IrRu(\eta^1\text{-}NC(H)C{=}CH_2)(CO)_3(\mu\text{-}CH_2)(dppm)_2][BF_4]$ (9). Method i. Compound **5** (60 mg. 0.047 mmol), Me_3NO (3.5 mg, 0.047 mmol), and acrylonitrile (0.1 mL, 1.5 mmol) were placed into a flask, and 3 mL of CH_2Cl_2 was added. The solution immediately became orange. After the mixture was stirred for 15 min, ether (20 mL) was added to precipitate an orange solid. The solid was then recrystallized from CH_2Cl_2/ether and dried in vacuo (85% yield). Anal. Calcd for $C_{57}H_{49}NBF_4O_3P_4IrRu$: C, 52.67; H, 3.80; N, 1.08%. Found: C, 51.65; H, 3.80; N, 1.34%.

Method ii. Compound **6** (0.0078 mmol) was prepared in situ in an NMR tube as described in part f in 0.5 mL of CD_2Cl_2, and 1 equiv of acrylonitrile (0.5 μL) was added. ^1H and ^{31}P NMR spectroscopy indicated complete conversion to **9**.

X-ray Data Collection. Yellow crystals of $[IrRuH(CO)_3(\mu\text{-}CO)(dppm)_2]\cdot 4.5C_6H_6$ (**2**) were obtained from slow diffusion of Et_2O into a benzene solution of the compound. Data were collected on a Bruker P4/RA/SMART 1000 CCD diffractometer[18] using Mo Kα radiation at −80 °C. Unit cell parameters were obtained from a least-squares refinement of the setting angles of 6209 reflections from the data collection. The lack of systematic absences and the diffraction symmetry indicated that the space group was $P1$ or $P\bar{1}$; the latter was established

(18) Programs for diffractometer operation, data reduction, and absorption correction were those supplied by Bruker.

by successful refinement of the structure. The data were corrected for absorption through use of Gaussian integration (indexing and measurement of crystal faces).

Yellow crystals of $[IrRu(CO)_3(\mu\text{-}CH_2)(\mu\text{-}CO)(dppm)_2][BF_4]\cdot CH_2Cl_2$ (**5**) were obtained from slow evaporation of a dichloromethane solution of the compound. A suitable crystal was immediately transferred to the cold nitrogen stream after removal from the mother liquor. Others deteriorated noticeably owing to solvent loss after 10 min. Data were collected on a Bruker P4/RA/SMART 1000 CCD diffractometer using Mo Kα radiation at −80 °C. Unit cell parameters were obtained from a least-squares refinement of the setting angles of 6519 reflections from the data collection. The space group was determined to be $P2_1/n$ (a nonstandard setting of $P2_1/c$ [No. 14]). The data were corrected for absorption through use of the SADABS procedure.

Light yellow crystals of $[IrRu(CO)_3(PMe_3)(\mu\text{-}CH_2)(dppm)_2][BF_4]\cdot 2CH_2Cl_2$ (**8**) were obtained from slow diffusion of Et_2O into a CH_2Cl_2 solution of the compound. Crystals again lost solvent quickly; therefore, they had to be mounted in the cold stream without delay. Data were collected on a Bruker P4/RA diffractometer using Cu Kα radiation at −60 °C. Unit cell parameters were obtained from a least-squares refinement of the setting angles of 44 reflections with $54.2° < 2\theta < 58.0°$. The monoclinic diffraction symmetry and systematic absences indicated the space group to be $P2_1/c$ (No. 14). The data were corrected for absorption through use of a semiempirical method (ψ scans of several high-χ reflections).

Structure Solution and Refinement. The structure of **2** was solved using direct methods (SHELXS-86),[19] and refinement was completed using the program SHELXL-93.[20] Hydrogen atoms were assigned positions on the basis of the geometries of their attached carbon atoms and were given thermal parameters 20% greater than those of the attached carbons. The metal atom positions were disordered such that one position (Ir/Ru′) was refined as an 85:15 combination of Ir and Ru, while the other (Ru/Ir′) was refined with the reverse ratio (85% Ru and 15% Ir). This disorder of the metals is accompanied by a disorder of hydride and one carbonyl group (C(3)O(3)) such that the primed atoms (H(1′), C(3′), and O(3′)) have 15% occupancies while the related unprimed atoms have 85% occupancies. The iridium−hydride distances (Ir−H(1) and Ir′−H(1′)) were fixed at 1.75 Å, and further restraints were applied to generate an idealized geometry for the hydride ligand H(1′): $d(P(2)\cdots H(1')) = d(P(4)\cdots H(1')) = 2.75$ Å; $d(C(2)\cdots H(1')) = d(C(4)\cdots H(1')) = 3.00$ Å. Distance restraints were also imposed upon the 15% occupancy carbonyl group (C(3′)O(3′)) attached to Ir′: $d(Ir'-C(3')) = 1.92$ Å; $d(O(3')-C(3')) = 1.15$ Å; $d(Ir'\cdots O(3')) = 3.07$ Å. The final model for **2** was refined to values of $R1(F) = 0.0365$ (for 11 250 data with $F_o^2 \geq 2\sigma(F_o^2)$) and $wR2(F^2) = 0.0973$ (for all 13 178 independent data).

The structure of **5** was solved using direct methods (SHELXS-86),[19] and refinement was completed using the program SHELXL-93.[20] Hydrogen atoms were assigned positions on the basis of the geometries of their attached carbon atoms and were given thermal parameters 20% greater than those of the attached carbons. The metal atom positions were disordered such that one position (Ir/Ru′) was refined as a 75:25 combination of Ir and Ru, while the other (Ru/Ir′) was refined with the reverse ratio (75% Ru and 25% Ir). The bridging methylene group (C(5)) and one carbonyl (C(4)O(4)) were found to be disordered over two sites in the same 75:25 ratio. As a result, there are two closely spaced positions for the methylene carbon with C(5) closer to Ir and C(5′) closer to Ir′. The distances of C(5′) to Ir′ (2.05 Å) and Ru′ (2.31 Å) were given fixed values on the basis of the corresponding Ir−C(5) and Ru−C(5) distances. Distances within the BF_4^- ion (F−B = 1.35 Å; F···F = 2.20 Å) and the disordered solvent CH_2Cl_2 molecule (Cl−C = 1.80 Å; Cl···Cl = 2.95 Å) were given fixed idealized values. The final model for **5** was refined to values of $R1(F) = 0.0549$ (for 6835 data with $F_o^2 \geq 2\sigma(F_o^2)$) and $wR2(F^2) = 0.1617$ (for all 11 017 independent data).

Scheme 1

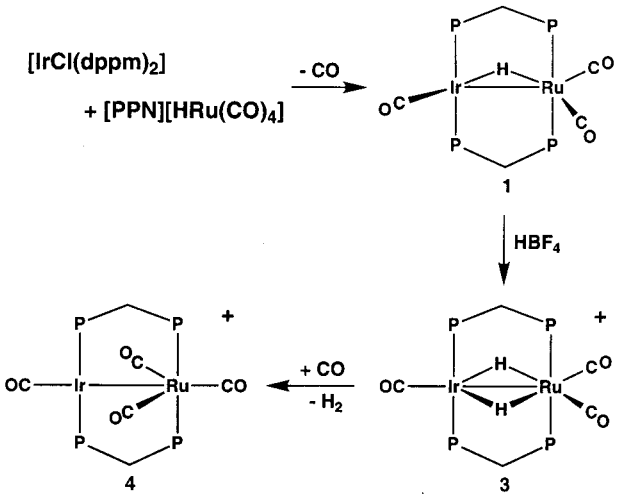

The structure of **7** was solved using direct methods (SHELXS-86),[19] and refinement was completed using the program SHELXL-93.[20] Hydrogen atoms were assigned positions on the basis of the geometries of their attached carbon atoms and were given thermal parameters 20% greater than those of the attached carbons. The final model for **7** was refined to values of $R1(F) = 0.0659$ (for 6167 data with $F_o^2 \geq 2\sigma(F_o^2)$) and $wR2(F^2) = 0.1739$ (for all 7345 independent data).

Crystallographic data for compounds **2**, **5**, and **7** are given in Table 2.

Results and Compound Characterization

In a previous study involving the RhOs combination of metals, the precursor compound used for the generation of methylene-containing species was the cationic tetracarbonyl $[RhOs(CO)_4(dppm)_2][BF_4]$.[13] The analogous IrRu complex has now been synthesized in a similar sequence of reactions, as outlined in Scheme 1. In the first step the heterobinuclear framework is constructed via chloride displacement from $[IrCl(dppm)_2]$ by the $[HRu(CO)_4]^-$ anion accompanied by unwinding of the chelating, Ir-bound dppm ligands into positions bridging both metals. The $^{31}P\{^1H\}$ NMR spectrum of the product, $[IrRu(CO)_3(\mu\text{-}H)(dppm)_2]$ (**1**), is characteristic of an AA′BB′ spin system in these dppm-bridged heterobinuclear systems.[16,21] The Ir-bound phosphine signal (δ 15.0) appears upfield from that of the Ru end (δ 48.4), as is typically observed for dppm complexes of these metals.[21−23] At −80 °C the NMR spectral data are consistent with the structure shown in Scheme 1. In the ^1H NMR spectrum the

(19) Sheldrick, G. M. *Acta Crystallogr.* **1990**, *A46*, 467.

(20) Sheldrick, G. M. SHELXL-93: Program for Crystal Structure Determination; University of Göttingen, Göttingen, Germany, 1993. Refinement was on F_o^2 for all reflections (having $F_o^2 \geq 3\sigma(F_o^2)$). The weighted R factor wR2 and goodness of fit S are based on F_o^2; the conventional R factor R1 is based on F_o, with F_o set to zero for negative F_o^2. The observed criterion of $F_o^2 > 2\sigma(F_o^2)$ is used only for calculating R1 and is not relevant to the choice of reflections for refinement. R factors based on F_o^2 are statistically about twice as large as those based on F_o, and R factors based on *all* data will be even larger.

(21) Antonelli, D. M.; Cowie, M. *Organometallics* **1990**, *9*, 1818.

(22) See for example: (a) Xiao, J.; Cowie, M. *Organometallics* **1993**, *12*, 463. (b) Xiao, J.; Santarsiero, B. D.; Vaartstra, B. A.; Cowie, M. *J. Am. Chem. Soc.* **1993**, *115*, 3212.

(23) Sterenberg, B. T.; Ph.D. Thesis, University of Alberta, Edmonton, AB, Canada, 1997; Chapter 5.

Table 2. Crystallographic Data for Compounds 2, 5, and 7

	$[IrRuH(CO)_4(dppm)_2]\cdot 4.5C_6H_6$ (**2**)	$[IrRu(CO)_4(\mu\text{-}CH_2)(dppm)_2][BF_4]\cdot CH_2Cl_2$ (**5**)	$[IrRu(PMe_3)(CO)_3(\mu\text{-}CH_2)(dppm)_2][BF_4]\cdot 2CH_2Cl_2$ (**7**)
formula	$C_{81}H_{72}IrO_4P_4Ru$	$C_{56}H_{48}BCl_2F_4IrO_4P_4Ru$	$C_{59}H_{59}BCl_4F_4IrO_3P_5Ru$
fw	1526.54	1359.80	1492.79
cryst dimens, mm	0.36 × 0.28 × 0.26	0.26 × 0.15 × 0.04	0.57 × 0.30 × 0.17
cryst syst	triclinic	monoclinic	monoclinic
space group	$P\bar{1}$ (No. 2)	$P2_1/n$ (nonstd setting of $P2_1/c$ (No. 14))	$P2_1/c$ (No. 14)
a, Å	14.0744(6)[a]	12.5470(7)[b]	20.356(2)[c]
b, Å	15.4510(7)	27.1409(13)	12.7687(11)
c, Å	17.6510(8)	15.9168(9)	23.221(2)
α, deg	89.8086(8)	90.0	90.0
β, deg	70.6204(8)	96.4809(10)	91.583(8)
γ, deg	74.9795(7)	90.0	90.0
V, Å^3	3482.8(3)	5385.6(5)	6033.2(9)
Z	2	4	4
d_{calcd}, g cm^{-3}	1.456	1.677	1.643
μ, mm^{-1}	2.267	3.027	9.583
diffractometer	Bruker P4/RA/SMART 1000 CCD[d]	Bruker P4/RA/SMART 1000 CCD[d]	Bruker P4/RA[d]
radiation (λ, Å)	graphite-monochromated Mo Kα (0.710 73)	graphite-monochromated Mo Kα (0.710 73)	graphite-monochromated Cu Kα (1.541 78)
T, °C	−80	−80	−60
scan type	ϕ rotations (0.3°)/ω scans (0.3°) (30 s exposures)	ϕ rotations (0.3°)/ω scans (0.3°) (30 s exposures)	ω
2θ(max), deg	51.40	52.82	115.0
no. of unique rflns	13 178	11 017	7345
no. of observns (NO)	11250 ($F_o^2 \geq 2\sigma(F_o^2)$)	6835 ($F_o^2 \geq 2\sigma(F_o^2)$)	6167 ($F_o^2 \geq 2\sigma(F_o^2)$)
range of abs cor factors	0.6416−0.4104	0.8943−0.5913	0.9873−0.3069
residual density e/Å^3	1.744 and −1.097	1.469 and −1.529	2.643 and − 2.124
R1 ($F_o^2 > 2\sigma(F_o^2)$)[e]	0.0365	0.0549	0.0659
wR2 (all data)	0.0973	0.1617	0.1739
GOF (S)[f]	1.040 ($F_o^2 \geq -3\sigma(F_o^2)$)	0.997 ($F_o^2 \geq -3\sigma(F_o^2)$)	1.074 ($F_o^2 \geq -3\sigma(F_o^2)$)

[a] Cell parameters obtained from least-squares refinement of 6209 centered reflections. [b] Cell parameters obtained from least-squares refinement of 6519 centered reflections. [c] Cell parameters obtained from least-squares refinement of 44 reflections with $54.2 < 2\theta < 58.0°$. [d] Programs for diffractometer operation, data reduction, and absorption correction were those supplied by Bruker. [e] $R1 = \sum||F_o| - |F_c||/\sum|F_o|$; $wR2 = [\sum w(F_o^2 - F_c^2)^2/\sum w(F_o^4)]^{1/2}$. [f] $S = [\sum w(F_o^2 - F_c^2)^2/(n-p)]^{1/2}$ (n = number of data; p = number of parameters varied; $w = [\sigma^2(F_o^2) + (a_oP)^2 + a_1P]^{-1}$, where $P = [\max(F_o^2, 0) = 2F_c^2]/3$). For **2** $a_o = 0.0494$ and $a_1 = 1.1045$; for **5** $a_o = 0.0812$ and $a_1 = 0.0$; for **7** $a_o = 0.1042$ and $a_1 = 45.2444$.

hydride resonance appears as an apparent quintet at δ −9.06, with essentially equal coupling (ca. 12 Hz) to both sets of inequivalent phosphorus nuclei, and the dppm methylene protons appear as two multiplets showing inequivalent environments on each side of the $IrRuP_4$ plane. The $^{13}C\{^1H\}$ NMR spectrum shows the expected three carbonyl resonances at δ 187.4, 212.0, and 223.5, with the high-field resonance corresponding to that bound to Ir. The proposed structure for **1** is similar to those suggested previously for the RhRu[23,24] and RhFe[21] analogues but differs from that proposed for the RhOs compound, in which the hydride is terminally bound to Os.[16] Apparently, in the RhOs compound the strong metal−hydride bond involving the late third-row metal[25] favors a terminal Os−H bond instead of a bridging interaction. As the temperature is raised, the spectral data for **1** indicate that a fluxional process is occurring that interchanges the two Ru-bound carbonyls. As a result, the $^{13}C\{^1H\}$ NMR spectrum at ambient temperature shows only two carbonyl resonances in a 1:2 ratio at δ 185.6 and 215.8, respectively, with the second resonance corresponding to the two Ru-bound carbonyls. The process that equilibrates both Ru-bound carbonyls probably occurs by an inversion of the "$(OC)Ir(\mu\text{-}H)Ru(CO)_2$" core (dppm groups above and below the plane of the drawing omitted), in which the hydride ligand moves between the two metals:

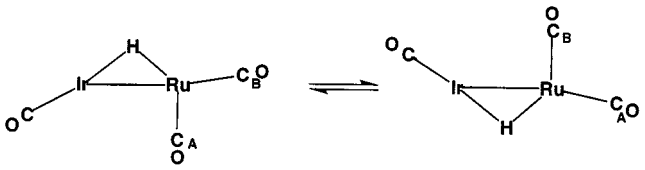

Also, as a result of this process, the environments on each side of the $IrRuP_4$ plane become averaged, resulting in a single resonance in the ^1H NMR spectrum for the four dppm methylene hydrogens. Such fluxionality is common for hydride- and dppm-bridged complexes.[21,26]

Conversion of **1** into $[IrRu(CO)_3(\mu\text{-}H)_2(dppm)_2][BF_4]$ (**3**) is readily accomplished by protonation with HBF_4, and this product appears to be exactly analogous to the known IrOs,[16] RhRu,[23,24] and RhOs[10] complexes. In **3** both bridging hydrides are chemically equivalent and appear as a triplet of triplets in the ^1H NMR spectrum at δ −8.87. The coupling of these hydrides to the Ir-bound phosphines ($^2J_{PH}$ = 13 Hz) is greater than that involving the Ru-bound phosphines ($^2J_{PH}$ = 7 Hz), presumably reflecting stronger interactions with the heavier metal. In the $^{13}C\{^1H\}$ NMR spectrum the Ir-bound carbonyl is at characteristically higher field than those on Ru (δ 175.5 (1C) vs 198.3 (2C)).

(24) Rowsell, B. D.; Sterenberg, B. T.; McDonald, R.; Cowie. M. To be submitted for publication.

(25) (a) Ziegler, T.; Tschinke, V. *Bonding Energetics in Organometallic Compounds*; American Chemical Society: Washington, DC, 1990; Chapter 19. (b) Ziegler, T. *Can. J. Chem.* **1995**, *73*, 743.

(26) (a) Antonelli, D. M.; Cowie, M. *Inorg. Chem.* **1990**, *17*, 2553. (b) McDonald, R.; Cowie, M. *Inorg. Chem.* **1990**, *29*, 1564. (c) Elliot, D. J.; Ferguson, G.; Holah, D. G.; Hughes, A. N.; Jennings, M.; Magnuson, V. R.; Potter, D.; Puddephatt, R. J. *Organometallics* **1990**, *9*, 1336.

Scheme 2

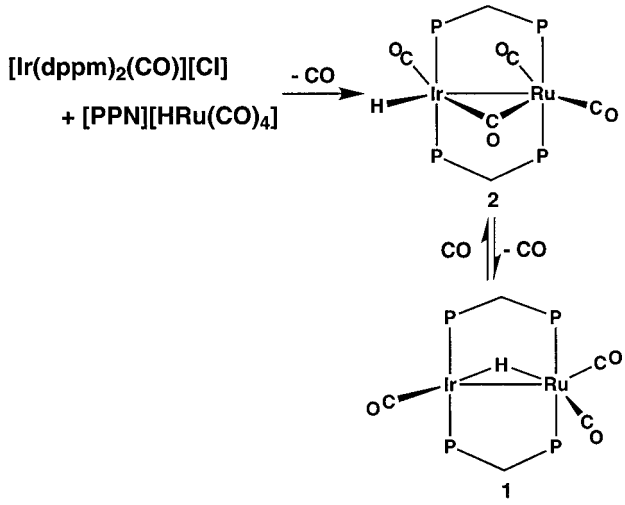

Reaction of **3** with CO results in H_2 displacement, yielding the targeted tetracarbonyl precursor [IrRu(CO)$_4$(dppm)$_2$][BF$_4$] (**4**), the structure of which is supported by all spectroscopic parameters; in particular, the highest field carbonyl resonance in the $^{13}C\{^1H\}$ NMR spectrum corresponds to that bound to Ir, while the low-field resonance corresponds to the two carbonyls on Ru that are bent toward Ir. A low-field shift of such carbonyls has previously been noted[27] and presumably reflects a weak interaction with the second metal. This interaction is clearly not strong enough to constitute a conventional bridging arrangement, since the IR spectrum shows only terminal carbonyl stretches (ν(CO): 1983, 1962 cm^{-1}). Compound **4** is analogous to the previously reported RhOs,[10] IrOs,[16] and RhRu[23,24] compounds.

The extreme air sensitivity of **1** and the resulting difficulties in handling this compound meant that the preparation of **4** by the route shown in Scheme 1 was unpredictable, often resulting in a number of unidentified decomposition products. Certainly the preparation of **4** by this route was much less convenient than the preparations of the analogous RhOs,[10] RhRu,[23,24] and RhFe[28] compounds. We therefore sought an alternate precursor to compound **4**. If instead of using [IrCl(dppm)$_2$] in the preparation of **1**, the carbonyl adduct [Ir(CO)(dppm)$_2$][Cl] is used, the *tetracarbonyl* compound [IrRu(H)(CO)$_3$(μ-CO)(dppm)$_2$] (**2**) is obtained, as shown in Scheme 2. Compound **2** can be converted to **1** by reaction with Me$_3$NO, and reaction of **1** with CO generates **2**. Compounds **1** and **2** have surprisingly different structures. At temperatures below −60 °C the $^{13}C\{^1H\}$ NMR spectrum of a ^{13}CO-enriched sample of **2** displays four signals, consistent with the structure shown in Scheme 2. At −105 °C, at which temperature all resonances are well-resolved, two carbonyls (δ 218.3, 207.8) are shown by selective ^{31}P-decoupling experiments to be bound terminally to Ru, while one (δ 189.1) is terminally bound to Ir, and the fourth (δ 262.7) is shown to bridge both metals, consistent with the low-frequency carbonyl stretch (1685 cm^{-1}) in the IR spectrum. The hydride resonance in the ^1H NMR spectrum appears as a triplet at δ −9.95 with coupling to only the Ir-bound phosphines, indicating that the hydride is bound terminally to this metal. This proposed structure has been confirmed by an X-ray determination, as shown in Figure 1. Bond lengths and angles are summarized in Table 3. Although the hydride ligand was not experimentally located, its approximate position is indicated by the vacant coordination site on Ir, falling between the carbonyl groups C(1)O(1) and C(2)O(2). Clearly, the carbonyl group C(1)O(1) is considerably removed from the site it would be expected to occupy opposite C(2), were the hydride ligand not present, and in fact C(1)O(1) occupies a position on Ir much like that of C(4)O(4) on Ru (compare: Ru−Ir−C(1) = 99.4(2)°, Ir−Ru−C(4) = 96.5(1)°). Each metal has a rather similar distorted octahedral geometry, in which the two octahedra are sharing an edge (Ir−Ru bond and bridging carbonyl), and the diphosphine ligands are mutually trans at each metal. The Ir−Ru distance (2.8091(3) Å) is normal for a single bond, and the carbonyl (C(2)O(2)) is essentially symmetrically bridged. The smaller steric requirement of the hydride ligand on Ir compared to the carbonyl in the related position on Ru gives rise to subtle geometrical differences at the two metals; therefore, the phosphines on Ir are bent toward the small hydride ligand (P(1)−Ir−P(3) = 167.34(4)°), whereas those on Ru are almost exactly trans (P(2)−Ru−P(4) = 176.95(4)°). The slightly shorter Ir−P distances compared to Ru−P probably also reflect the less crowded environment at the heavier metal. All other parameters within the complex appear normal.

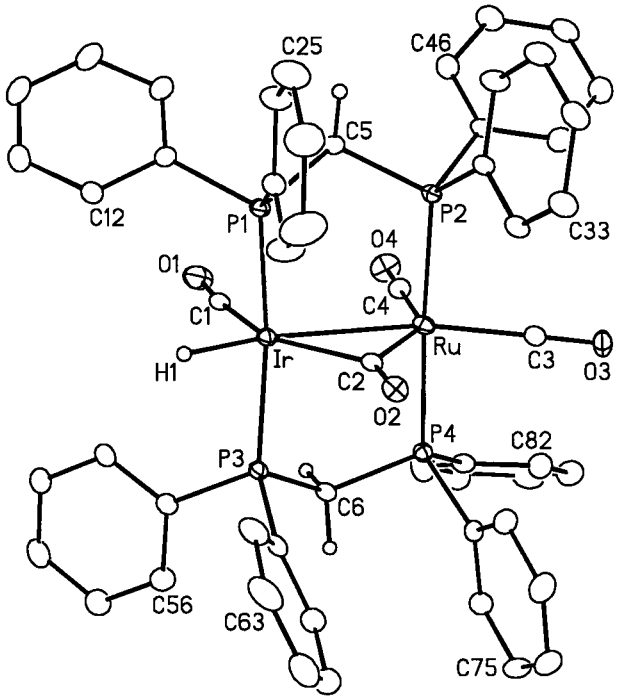

Figure 1. Perspective view of [IrRuH(CO)$_3$(μ-CO)(dppm)$_2$] (**2**) showing the atom-labeling scheme. Non-hydrogen atoms are represented by Gaussian ellipsoids at the 20% probability level. The hydride and dppm methylene hydrogen atoms are shown with arbitrarily small thermal parameters, while the dppm phenyl hydrogens are not shown. Atom H(1) was not located but was placed in an idealized position, as described in the text.

Compound **2** is shown to undergo two fluxional processes in solution. A spin-saturation-transfer experiment at −60 °C shows that the terminal, Ir-bound

(27) George, D. S. A.; McDonald, R.; Cowie, M. *Organometallics* **1998**, *17*, 2553.
(28) Lo, J. M. H.; Cowie, M. Unpublished results.

Table 3. Selected Bond Lengths and Angles for Compound 2

(a) Distances (Å)

Ir−Ru	2.8091(3)	P(4)−C(6)	1.848(4)
Ir−P(1)	2.3029(10)	O(1)−C(1)	1.115(5)
Ir−P(3)	2.3117(10)	O(2)−C(2)	1.188(5)
Ir−C(1)	1.935(4)	O(3)−C(3)	1.148(6)
Ir−C(2)	2.063(4)	O(4)−C(4)	1.112(5)
Ru−P(2)	2.3361(10)	P(1)−C(11)	1.830(4)
Ru−P(4)	2.3360(10)	P(1)−C(21)	1.834(4)
Ru−C(2)	2.117(4)	P(2)−C(31)	1.828(4)
Ru−C(3)	1.925(5)	P(2)−C(41)	1.832(4)
Ru−C(4)	1.954(4)	P(3)−C(51)	1.845(4)
P(1)−C(5)	1.830(4)	P(3)−C(61)	1.823(4)
P(2)−C(5)	1.840(4)	P(4)−C(81)	1.835(4)
P(3)−C(6)	1.831(4)	P(4)−C(81)	1.839(4)

(b) Angles (deg)

Ru−Ir−P(1)	94.62(3)	P(2)−Ru−C(4)	89.65(12)
Ru−Ir−P(3)	94.31(3)	P(4)−Ru−C(2)	89.96(10)
Ru−Ir−C(1)	99.36(12)	P(4)−Ru−C(3)	87.20(14)
Ru−Ir−C(2)	48.60(11)	P(4)−Ru−C(4)	91.54(12)
Ru−Ir−H(1)[a]	157	C(2)−Ru−C(3)	104.68(18)
P(1)−Ir−P(3)	167.34(4)	C(2)−Ru−C(4)	143.47(16)
P(1)−Ir−C(1)	90.54(11)	C(3)−Ru−C(4)	111.8(2)
P(1)−Ir−C(2)	91.81(10)	Ir′−Ru′−C(3′)[b]	144.8(7)
P(3)−Ir−C(1)	96.84(11)	P(1)−Ru′−C(3′)	84.7(9)
P(3)−Ir−C(2)	87.39(10)	P(3)−Ru′−C(3′)	82.8(9)
C(1)−Ir−C(2)	147.96(16)	C(1)−Ru′−C(3′)	115.9(7)
C(1)−Ir−H(1)[a]	104	C(2)−Ru′−C(3′)	96.2(7)
C(2)−Ir−H(1)[a]	108	Ir−C(1)−O(1)	174.4(4)
Ir−Ru−P(2)	90.87(3)	Ir−C(2)−Ru	84.43(14)
Ir−Ru−P(4)	91.78(3)	Ir−C(2)−O(2)	138.8(3)
Ir−Ru−C(2)	46.97(10)	Ru−C(2)−O(2)	136.7(3)
Ir−Ru−C(3)	151.65(15)	Ru−C(3)−O(3)	178.7(5)
Ir−Ru−C(4)	96.50(12)	Ru−C(4)−O(4)	178.1(4)
P(2)−Ru−P(4)	176.95(4)	P(1)−C(5)−P(2)	111.3(2)
P(2)−Ru−C(2)	90.76(10)	P(3)−C(6)−P(4)	112.80(19)
P(2)−Ru−C(3)	89.75(14)		

[a] Atom H(1) was refined with the constraints described in the Experimental Section. [b] Primed atoms refer to the minor occupant (15%) in the disordered structure, which were refined with the distance restraints given in the Experimental Section.

carbonyl and the bridging carbonyl are exchanging, as are the two on Ru. We propose the process

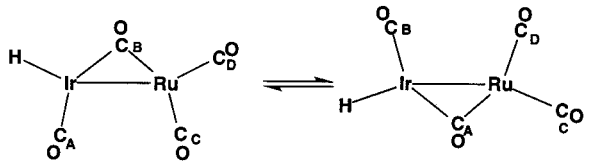

for this exchange (phosphines above and below the plane of the paper are not shown), in which CO_A and CO_B interchange, as do CO_C and CO_D. At 10 °C the four ^{13}CO signals have coalesced into two broad, unresolved signals at δ 225.7 and 212.2, corresponding to the averaging of the respective pairs of carbonyls as described above. At this temperature spin-saturation-transfer experiments show an additional process in which all carbonyls are exchanging, and warming the sample to 50 °C results in coalescence of these signals into one at δ 217.4. At all temperatures above −60 °C the hydride resonance appears as an unresolved signal. The second process that equilibrates all four carbonyls presumably involves a merry-go-round motion of all carbonyls and the hydride, in which these ligands move around the Ir−Ru core in the plane perpendicular to the phosphines, passing from metal to metal.

Compound **2** can also be used in the preparation of **3**, except that protonation in this case is accompanied by loss of a carbonyl. As a result, this route always generates a mixture of **3** and **4**, with the CO generated in the protonation of **2** converting some of **3** into **4**. Under a CO atmosphere, this mixture of **3** and **4** is converted cleanly to **4**. Owing to its much greater ease of handling compared to compound **1**, the tetracarbonyl hydride (**2**) is the precursor of choice for the preparation of **4**.

As in the RhOs chemistry,[13] the tetracarbonyl complex **4** serves as a convenient precursor for methylene-containing species. Therefore, the reaction of **4** with diazomethane generates the methylene-bridged $[IrRu(CO)_4(\mu\text{-}CH_2)(dppm)_2][BF_4]$ (**5**) as diagrammed in Scheme 3. In the ^1H NMR spectrum the μ-CH_2 group appears as a triplet of triplets at δ 3.57, with the coupling to the Ir-bound phosphines ($^3J_{PH}$ = 23 Hz) being greater than that involving the Ru-bound phosphines ($^3J_{PH}$ = 11 Hz). The dppm methylene protons appear at δ 3.08 and 3.87 and are readily differentiated from the metal-bound CH_2 group by their characteristic appearance (AB quartet with superimposed phosphorus coupling) and by the broad-band ^{31}P-decoupled ^1H NMR spectrum in which the dppm methylenes collapse to the expected AB quartet while the metal-bridged CH_2 group appears as a singlet. In the $^{13}C\{^1H\}$ NMR spectrum the carbonyls

Scheme 3

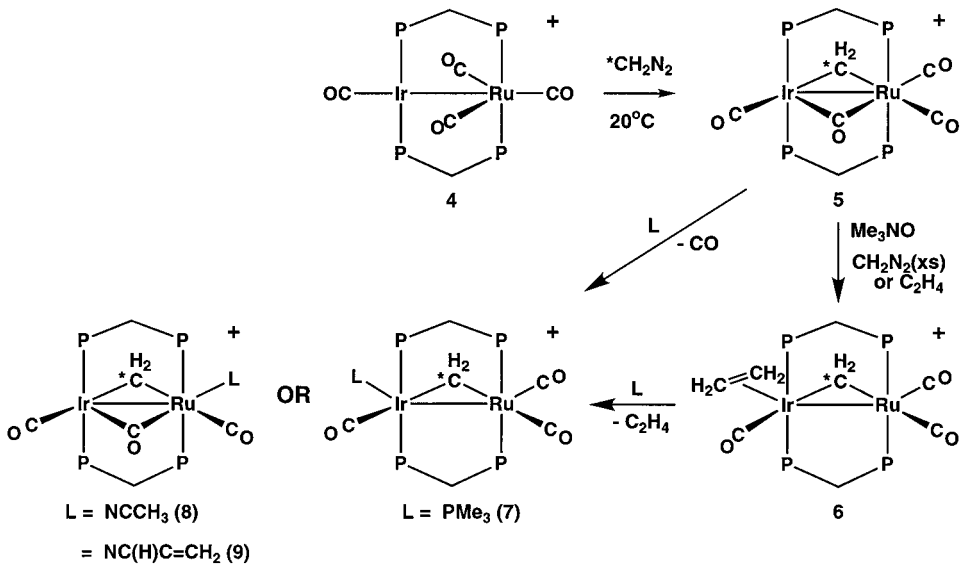

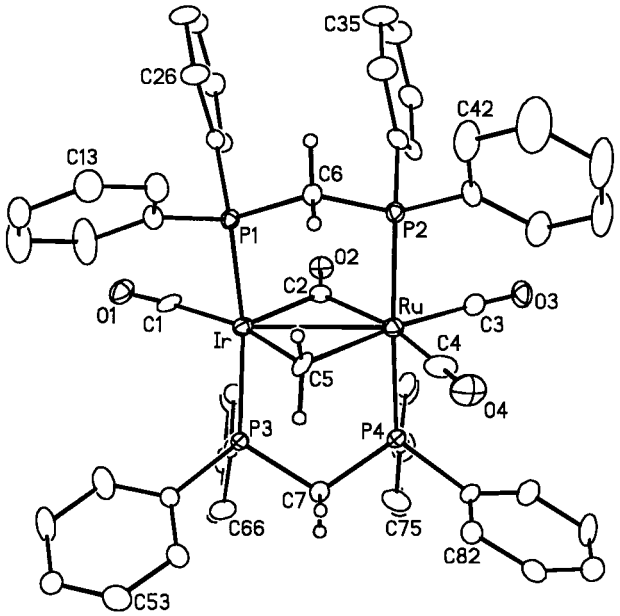

Figure 2. Perspective view of the $[IrRu(CO)_3(\mu\text{-}CH_2)(\mu\text{-}CO)(dppm)_2]^+$ cation of complex **5** showing the atom-labeling scheme. Thermal parameters are as described for Figure 1.

appear as four separate resonances. The low-field signal (δ 211.3) for the bridging carbonyl appears as a doublet of multiplets with coupling to all ^{31}P nuclei and 23 Hz coupling to the Ru-bound carbonyl at δ 191.7, indicating that these carbonyls are mutually trans. The chemical shifts of the remaining carbonyls are somewhat anomalous, with the low-field shift corresponding to the Ir-bound CO (in all other compounds the Ir-bound carbonyls appear at higher field than those on Ru). All ^{13}C NMR assignments have been confirmed by selective ^{31}P-decoupling experiments.

The structure of **5** has been determined by X-ray techniques in order to establish whether the bridging carbonyl has a conventional geometry or is semibridging, since the carbonyl stretch (1783 cm^{-1}) is consistent with either interpretation. In addition, it was deemed necessary to fully characterize this methylene-bridged species, since subtle differences between it and the RhOs analogue may offer clues to their reactivity differences (vide infra). The structure shown in Figure 2 together with the parameters given in Table 4 clearly show a conventional bridging carbonyl with a normal accompanying metal−metal bond (2.8650(7) Å). This bridging carbonyl (C(2)O(2)) is slightly asymmetrically bonded to the metals, as seen by the somewhat shorter Ir−carbon distance (Ir−C(2) = 2.033(8) Å, Ru−C(2) = 2.072(8) Å), but is shown to be conventionally bridged rather than semibridged by the close-to-symmetric angles at the carbonyl (Ir−C(2)−O(2) = 134.4(7)°, Ru−C(2)−O(2) = 137.1(7)°). The methylene group, on the other hand, shows significant asymmetry in its bonding to both metals, being more strongly bound to Ir (Ir−C(5) = 2.045(11) Å) than to Ru (Ru−C(5) = 2.305(12) Å). This observed asymmetry is consistent with the larger coupling of the methylene group to the Ir-bound phosphines in the ^1H NMR spectrum (vide supra). The differences in geometries at both metals result primarily from the additional carbonyl bound to Ru and the resulting greater crowding at this metal.

Table 4. Selected Bond Lengths and Angles for Compound 5

(a) Distances (Å)

Ir−Ru	2.8650(7)	Ru−C(5)	2.305(12)
Ir−P(1)	2.3516(19)	Ru′−C(4′)	2.17(5)
Ir−P(3)	2.3503(19)	Ru′−C(5′)	2.31[†]
Ir−C(1)	1.868(9)	O(1)−C(1)	1.141(10)
Ir−C(2)	2.033(8)	O(2)−C(2)	1.194(9)
Ir−C(5)	2.045(11)	O(3)−C(3)	1.119(10)
Ir′−C(5′)[a]	2.05[b]	O(4)−C(4)	1.155(13)
Ru−P(2)	2.3726(19)	O(4′)−C(4′)	1.17(5)
Ru−P(4)	2.361(2)	P(1)−C(6)	1.834(8)
Ru−C(2)	2.072(8)	P(2)−C(6)	1.837(8)
Ru−C(3)	1.916(10)	P(3)−C(7)	1.848(8)
Ru−C(4)	1.981(12)	P(4)−C(7)	1.838(8)

(b) Angles (deg)

Ru−Ir−P(1)	93.31(5)	P(4)−Ru−C(5)	90.8(5)
Ru−Ir−P(3)	92.76(5)	C(2)−Ru−C(3)	99.3(3)
Ru−Ir−C(1)	145.5(3)	C(2)−Ru−C(4)	162.1(5)
Ru−Ir−C(2)	46.3(2)	C(2)−Ru−C(5)	90.2(3)
Ru−Ir−C(5)	52.9(3)	C(3)−Ru−C(4)	98.5(5)
P(1)−Ir−P(3)	165.59(7)	C(3)−Ru−C(5)	170.5(4)
P(1)−Ir−C(1)	91.3(2)	C(4)−Ru−C(5)	72.1(5)
P(1)−Ir−C(2)	96.5(2)	Ir′−Ru′−C(4′)	121(2)
P(1)−Ir−C(5)	86.0(5)	Ir′−Ru′−C(5′)	45.11(13)
P(3)−Ir−C(1)	91.1(2)	P(1)−Ru′−C(4′)	82.7(11)
P(3)−Ir−C(2)	97.1(2)	P(1)−Ru′−C(5′)	89.2(18)
P(3)−Ir−C(5)	87.3(5)	P(3)−Ru′−C(4′)	83.0(11)
C(1)−Ir−C(2)	99.2(4)	P(3)−Ru′−C(5′)	85.9(18)
C(1)−Ir−C(5)	161.7(5)	C(1)−Ru′−C(4′)	94(2)
C(2)−Ir−C(5)	99.1(4)	C(1)−Ru′−C(5′)	169.3(4)
Ru′−Ir′−C(5′)[a]	52.96(15)	C(2)−Ru′−C(4′)	167(2)
P(2)−Ir′−C(5′)	92(2)	C(2)−Ru′−C(5′)	91.4(3)
P(4)−Ir′−C(5′)	88(2)	C(4′)−Ru′−C(5′)	76(2)
C(2)−Ir′−C(5′)	98.1(3)	Ir−P(1)−C(6)	112.6(2)
C(3)−Ir′−C(5′)	162.3(4)	Ru−P(2)−C(6)	111.5(2)
Ir−Ru−P(2)	91.14(5)	Ir−P(3)−C(7)	113.4(3)
Ir−Ru−P(4)	91.46(6)	Ru−P(4)−C(7)	112.4(3)
Ir−Ru−C(2)	45.2(2)	Ir−C(1)−O(1)	174.3(9)
Ir−Ru−C(3)	144.5(3)	Ir−C(2)−Ru	88.5(3)
Ir−Ru−C(4)	117.1(4)	Ir−C(2)−O(2)	134.4(7)
Ir−Ru−C(5)	45.0(3)	Ru−C(2)−O(2)	137.1(7)
P(2)−Ru−P(4)	176.76(8)	Ru−C(3)−O(3)	177.2(8)
P(2)−Ru−C(2)	90.8(2)	Ru−C(4)−O(4)	177.3(14)
P(2)−Ru−C(3)	90.7(2)	Ru′−C(4′)−O(4′)	163(7)
P(2)−Ru−C(4)	87.1(3)	Ir−C(5)−Ru	82.1(4)
P(2)−Ru−C(5)	89.7(5)	Ir′−C(5′)−Ru′	81.93(17)
P(4)−Ru−C(2)	92.4(2)	P(1)−C(6)−P(2)	112.8(4)
P(4)−Ru−C(3)	88.3(2)	P(3)−C(7)−P(4)	111.4(4)
P(4)−Ru−C(4)	90.0(3)		

[a] Primed atoms are those of the 25% disorder. [b] Distance fixed during refinement.

Although **5** does not react further with diazomethane at ambient temperature, removal of a carbonyl with trimethylamine oxide followed by addition of CH_2N_2 does lead to further "CH_2" incorporation to yield the methylene-bridged, ethylene complex $[IrRu(C_2H_4)(CO)_3(\mu\text{-}CH_2)(dppm)_2][BF_4]$ (**6**). At ambient temperature the ^1H NMR signal for the methylene group of **6** appears as a triplet of triplets at δ 6.20, displaying comparable coupling to the Ir- and Ru-bound phosphines ($^3J_{PH}$ = 8, 10 Hz, respectively); the signals due to the ethylene group are not observed at this temperature. At −80 °C the ethylene signals appear as broad singlets in the ^1H NMR spectrum at δ 1.73 and δ 0.54, which sharpen slightly upon decoupling of the Ir-bound ^{31}P signal, suggesting the structure shown in Scheme 3, in which the ethylene is bound to Ir. In addition, selective ^{31}P decoupling of the three ^{13}CO resonances indicates that two carbonyls are bound to Ru and one is bound to Ir. The presence of two carbonyls on Ru, together with the methylene group and the pair of phosphines, argues

against the olefin also being on this metal, owing to the steric crowding that would result. The breadth of the ethylene ^{1}H resonances can be attributed to two fluxional processes, both of which have been investigated using spin-saturation-transfer experiments. Irradiating either ethylene resonance at temperatures between −60 and −90 °C results in a decrease in intensity of the other, indicating an exchange between the two environments, characteristic of ethylene rotation. The rates of rotation have been determined at four temperatures between −70 and −87 °C by selective inversion recovery ^{1}H NMR experiments,[29] yielding $\Delta H^{\ddagger} = 10.0 \pm 1.8$ kcal/mol and $\Delta S^{\ddagger} = -2.3 \pm 9.1$ cal/(mol K) for this process. Above −65 °C the second process becomes significant, involving the exchange of coordinated ethylene with free ethylene in solution. This exchange process has also been confirmed by a spin-saturation-transfer experiment in the presence of excess ethylene.

To determine the fate of the methylene group in the transformation of **5** to **6**, the labeled compound [IrRu(CO)$_4$(^{13}CH$_2$)(dppm)$_2$][BF$_4$] (**5-^{13}C**) was reacted with unlabeled CH_2N_2 after brief reaction with Me_3NO. On the basis of the ^{1}H NMR spectrum, which shows the μ-CH$_2$ resonance primarily as a doublet of multiplets ($^1J_{CH} = 140$ Hz) with approximately 10% of a superimposed resonance resulting from $^{12}CH_2$, the majority of the label (≃90%) is seen to remain in the bridging methylene group. This means that approximately 10% of the $^{13}CH_2$ label has been incorporated into the ethylene produced, either coordinated to Ir or existing as a free ethylene. Integration of the ^{1}H NMR signals of the reaction mixture shows that approximately 1.2 equiv of free ethylene is present in solution.

The ^{13}C{^{1}H} NMR resonances for the bridging methylene and the ethylene carbons of compound **6** appear as singlets at δ 64.3, 26.4, and 22.6, respectively, and show no coupling to the ^{31}P nuclei. Both ethylene resonances are extremely weak, owing to the small amount of ^{13}C incorporation into this group.

Compound **6** can also be independently synthesized by the reaction of **5** with ethylene in the presence of trimethylamine oxide. To establish whether the ethylene produced in the above reaction with diazomethane was generated by the presumed tricarbonyl species [IrRu(CO)$_3$(μ-CH$_2$)(dppm)$_2$][BF$_4$] or was independently produced in solution and subsequently bound to this unsaturated product, a blank experiment was carried out under identical conditions except in the absence of complex **5**. The absence of ethylene in this experiment confirms that an IrRu species is responsible for ethylene formation.

In the absence of excess ethylene, the labile ethylene ligand in **6** is readily lost, yielding several unidentified decomposition products. Not surprisingly, this ligand can also be displaced by ligands such as acetonitrile, trimethylphosphine, and acrylonitrile. However, two structural types are obtained. In the case of the PMe_3 adduct, [IrRu(PMe_3)(CO)$_3$(μ-CH$_2$)(dppm)$_3$][BF$_4$] (**7**), the spectral parameters are in good agreement with those of the ethylene adduct (**6**), and it is assumed to have a similar structure in which the ethylene ligand has been displaced by PMe_3. In particular, the ^{31}P{^{1}H} resonances for the dppm groups are very similar in the two compounds, with those corresponding to the Ru-bound nuclei being almost superimposable, while that of the Ir-bound nuclei of **7** is ca. 7 ppm upfield of the comparable resonance in **6**, consistent with the substitution of the ethylene ligand on Ir by the more basic PMe_3 group. The ^{1}H resonance for the bridging methylene group (δ 4.17) shows the expected coupling to the three chemically inequivalent sets of phosphorus nuclei (two dppm ^{31}P nuclei on Ir, two on Ru, and the PMe_3 group), and the upfield shift compared to that of the ethylene adduct (**6**) is again consistent with replacement of ethylene by PMe_3. The coupling patterns involving the ^{31}P and ^{13}CO nuclei in **7** are somewhat unusual. Although the PMe_3 group is bound to Ir, it couples equally strongly to all four dppm ^{31}P nuclei; this means that the $^3J_{PP}$ value, which is a measure of the coupling between the PMe_3 on Ir and the dppm ^{31}P nuclei on Ru, is essentially the same as the $^2J_{PP}$ value between the PMe_3 and the dppm phosphorus nuclei bound to Ir. In a related complex, [IrRh(CH_3)(CO)$_2$(PMe_3)(dppm)$_2$][CF_3SO_3],[30] the Ir-bound PMe_3 group displayed no P−P coupling to the adjacent Ir-bound dppm nuclei but displayed 15 Hz coupling to the remote dppm groups on Rh. In addition, the ^{13}C{^{1}H} NMR spectrum of **7** shows that the Ir-bound carbonyl has the expected coupling to PMe_3 and to the adjacent ends of the dppm ligands, whereas one Ru-bound carbonyl displays coupling to only the adjacent dppm ^{31}P nuclei. However, the second Ru-bound carbonyl shows coupling to the adjacent ^{31}P nuclei of dppm *and* 20 Hz coupling to the remote PMe_3 group; the large magnitude of this latter P−C coupling presumably results from their arrangements essentially opposite the Ir−Ru bond (vide infra). Strong magnetic coupling through a metal−metal bond has previously been observed.[30,31] Despite these NMR spectral anomalies, much of the connectivity can still be established from the P−C coupling between the dppm groups and the carbonyls. Any uncertainty in the position of the PMe_3 group is overcome by the X-ray structure determination, which is shown in Figure 3 and which clearly shows the PMe_3 group bound to Ir. Selected bond lengths and angles are given in Table 5. This structure is not unlike that shown previously for compound **2** (Figure 1), having two edge-shared octahedra shared along the metal−metal bond and the bridging methylene group. The steric demands of the PMe_3 group are manifest in a bending of the dppm ligands on both metals away from the PMe_3 group (P(1)−Ir−P(3) = 165.86(9)°, P(2)−Ru−P(4) = 160.9(1)°). The Ir−Ru distance (2.8892(9) Å) is consistent with a single bond, and the geometry of the bridging methylene group is essentially symmetric and unexceptional. The short Ir−C(1)O(1) distance (1.859(12) Å) is consistent with more π back-donation to this carbonyl as a result of the strong donor ability of the adjacent PMe_3 group. Surprisingly, perhaps, the Ru−C(2)O(2) distance (1.859(13) Å) is also short (compare Ru−C(3)O(3) = 1.931(11)

(29) Data analysis was carried out according to the method of McClung and co-workers: Muhandiram, D. R.; McClung, R. E. D. *J. Magn. Reson.* **1987**, *71*, 187.

(30) Oke, O.; McDonald, R.; Cowie, M. *Organometallics* **1999**, *18*, 1629.

(31) (a) Vaartstra, B. A.; Xiao, J.; Jenkins, J. A.; Verhagen, R.; Cowie, M. *Organometallics* **1991**, *10*, 2708. (b) Antwi-Nsiah, F. H.; Torkelson, J. R.; Cowie, M. *Inorg. Chim. Acta* **1997**, *259*, 213. (c) Mague, J. T. *Organometallics* **1986**, *5*, 918. (d) Brown, M. P.; Fisher, J. R.; Hill, R. H.; Puddephatt, R. J.; Seddon, R. R. *Inorg. Chem.* **1981**, *20*, 2516.

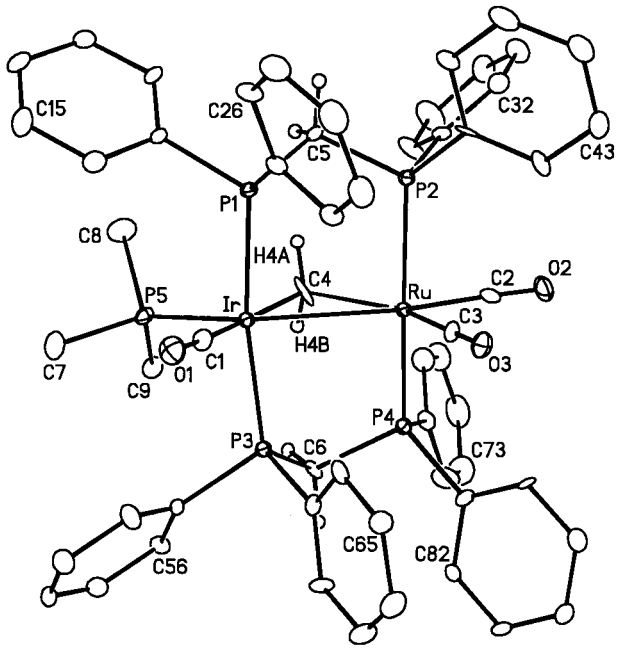

Figure 3. Perspective view of the $[IrRu(PMe_3)(CO)_3(\mu\text{-}CH_2)(dppm)_2]^+$ cation of complex **7** showing the atom-labeling scheme. Thermal parameters are as described for Figure 1.

Table 5. Selected Bond Lengths and Angles for Compound 7

(a) Distances (Å)

Ir−Ru	2.8892(9)	P(1)−C(5)	1.837(11)
Ir−P(1)	2.347(3)	P(2)−C(5)	1.824(10)
Ir−P(3)	2.329(3)	P(3)−C(6)	1.826(10)
Ir−P(5)	2.366(3)	P(4)−C(6)	1.838(10)
Ir−C(1)	1.859(12)	P(5)−C(7)	1.807(13)
Ir−C(4)	2.152(11)	P(5)−C(8)	1.816(13)
Ru−P(2)	2.352(3)	P(5)−C(9)	1.790(11)
Ru−P(4)	2.373(3)	O(1)−C(1)	1.168(13)
Ru−C(2)	1.859(13)	O(2)−C(2)	1.159(14)
Ru−C(3)	1.931(11)	O(3)−C(3)	1.133(12)
Ru−C(4)	2.175(13)		

(b) Angles (deg)

Ru−Ir−P(1)	88.87(7)	P(2)−Ru−C(4)	85.1(4)
Ru−Ir−P(3)	85.16(7)	P(4)−Ru−C(2)	84.9(3)
Ru−Ir−P(5)	130.69(7)	P(4)−Ru−C(3)	101.1(4)
Ru−Ir−C(1)	125.3(3)	P(4)−Ru−C(4)	85.8(4)
Ru−Ir−C(4)	48.5(3)	C(2)−Ru−C(3)	95.6(5)
P(1)−Ir−P(3)	165.86(9)	C(2)−Ru−C(4)	116.8(5)
P(1)−Ir−P(5)	99.15(10)	C(3)−Ru−C(4)	147.5(4)
P(1)−Ir−C(1)	85.7(4)	Ir−P(1)−C(5)	114.3(4)
P(1)−Ir−C(4)	89.9(4)	Ru−P(2)−C(5)	114.6(4)
P(3)−Ir−P(5)	94.45(9)	Ir−P(3)−C(6)	113.1(4)
P(3)−Ir−C(1)	87.3(4)	Ru−P(4)−C(6)	113.2(4)
P(3)−Ir−C(4)	95.6(4)	Ir−P(5)−C(7)	116.2(4)
P(5)−Ir−C(1)	103.9(3)	Ir−P(5)−C(8)	118.6(4)
P(5)−Ir−C(4)	82.8(3)	Ir−P(5)−C(9)	117.2(4)
C(1)−Ir−C(4)	172.6(4)	C(7)−P(5)−C(8)	101.6(7)
Ir−Ru−P(2)	93.06(7)	C(7)−P(5)−C(9)	101.7(6)
Ir−Ru−P(4)	93.25(7)	C(8)−P(5)−C(9)	98.5(6)
Ir−Ru−C(2)	164.5(4)	Ir−P(5)−C(1)−O(1)	177.5(11)
Ir−Ru−C(3)	99.8(3)	Ru−C(2)−O(2)	178.4(11)
Ir−Ru−C(4)	47.8(3)	Ru−C(3)−O(3)	179.2(9)
P(2)−Ru−P(4)	160.86(10)	Ir−C(4)−Ru	83.8(5)
P(2)−Ru−C(2)	84.2(3)	P(1)−C(5)−P(2)	110.0(6)
P(2)−Ru−C(3)	95.6(4)	P(3)−C(6)−P(4)	107.2(5)

Å), and this may result from a transmission of electronic effects from the PMe_3 group through the Ir−Ru bond, to which both groups are mutually trans. All other parameters within the complex cation appear normal.

The acetonitrile adduct $[IrRu(NCCH_3)(CO)_2(\mu\text{-}CO)(\mu\text{-}CH_2)(dppm)_2][BF_4]$ (**8**) is stoichiometrically analogous to compounds **6** and **7**, having an acetonitrile group instead of the ethylene and PMe_3 ligands, respectively. However, the structure of **8** appears to differ substantially from those of **6** and **7**, instead resembling the structure observed for **5**. This is most clearly seen in the IR and $^{31}P\{^1H\}$ NMR spectra. Unlike compounds **6** and **7**, which show only terminal carbonyl bands in the IR spectra, **8** displays a band at 1745 cm^{-1}, corresponding to a bridging carbonyl stretch. This compares well to the analogous stretch for **5**, observed at 1783 cm^{-1}. In addition, the $^{31}P\{^1H\}$ NMR spectrum of **8** has both sets of resonances (Ru- and Ir-bound ^{31}P nuclei) substantially downfield from those in **6** and **7** but in closer proximity to the resonances for **5**. If **8** had a geometry analogous to those of **6** and **7**, with the NCMe group bound to Ir, we would have expected a change in the resonances for the Ir-bound ^{31}P nuclei, owing to the different ligands on Ir, but would have expected the resonances for the Ru-bound ^{31}P nuclei to be closely comparable, having an identical ligand set at this metal. Instead, the Ru-bound ^{31}P resonances for **6** and **7** are approximately 14 ppm upfield from those of **8**. In addition, the $^{13}C\{^1H\}$ resonances for the carbonyls in **8** are comparable to those in **5**, apart from the absence of the fourth resonance of **5** at δ 191.7. In **5** this carbonyl resonance displays 23 Hz coupling to the bridging carbonyl, since they are mutually trans; the absence of similar coupling in **8** identifies the site of the acetonitrile ligand as opposite the bridging carbonyl, as shown in Scheme 3.

Despite the lability of the ethylene ligand in **6**, attempts to displace this group by other olefins (acrylonitrile, dimethyl maleate, methyl acrylate) succeeded only with acrylonitrile, yielding $[IrRu(\eta^1\text{-}NC(H)C{=}CH_2)(CO)_2(\mu\text{-}CH_2)(\mu\text{-}CO)(dppm)_2][BF_4]$ (**9**). However, it appears that the acrylonitrile is not bound through the olefinic moiety, as in most low-valent, late-metal complexes,[32] but is N-bound through the nitrile functionality to give a product that spectroscopically is very similar to the acetonitrile adduct (**8**). Apart from the close similarity in the spectral parameters of **8** and **9** additional support for the N-bound formulation is obtained from the ^1H NMR spectrum, in which the olefin protons are essentially unperturbed from those of the uncomplexed olefin, in contrast to those of the ethylene ligand in **6** which are shifted substantially upfield from free ethylene. No band is observed in the IR spectrum for

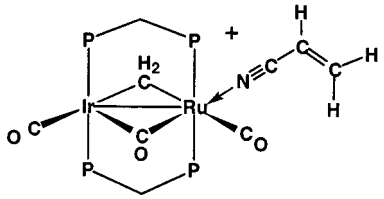

(9)

(32) See for example: (a) Grant, S. M.; Manning, A. R. *J. Chem. Soc., Dalton Trans.* **1979**, 1789. (b) Connelly, N. G.; Kelly, R. L.; Whiteley, M. W. *J. Chem. Soc., Dalton Trans.* **1981**, 34. (c) Werner, H.; Juthani, B. *J. Organomet. Chem.* **1981**, 209, *211*. (d) Albers, M. O.; Colville, N. J.; Singleton, E. *J. Chem. Soc., Dalton Trans.* **1982**, 1069. (e) Ashton, H. C.; Manning, A. R. *Inorg. Chem.* **1983**, *22*, 1440. (f) Morrow, J. R.; Tonker, T. L.; Templeton, J. L. *J. Am. Chem. Soc.* **1985**, *107*, 6957 and references therein.

the olefin functionality; this is not surprising, since the C═C stretch is also very weak in the free olefin. The C≡N stretch for **9** was observed as a very weak band at 2150 cm^{-1}; by comparison, no peak attributable to ν(CN) was observed for the acetonitrile adduct **8**. Although this bonding mode for cyano olefins is uncommon for the heavier late transition metals, it has been observed[33] in complexes of Os(II) and Ir(I); in the latter case the bridging TCNE ligand is a dianionic group. This bonding mode is relatively common with lighter metals having a preference for hard ligands.[34]

Discussion

The incorporation of a methylene group into [IrRu(CO)$_4$(dppm)$_2$][BF$_4$] (**4**) is readily accomplished by reaction with diazomethane at ambient temperature, yielding the methylene-bridged [IrRu(CO)$_4$(μ-CH$_2$)(dppm)$_2$][BF$_4$] (**5**) as the sole product. The direct synthesis of methylene-bridged complexes via reactions of the appropriate complexes with diazomethane is well-established.[13,35] The failure of **4** to incorporate more than a single methylene unit is in contrast to the ambient-temperature reaction involving the RhOs analogue in which *four* methylene groups are incorporated, giving the C_3- and C_1-containing product, [RhOs(η^1-C$_3$H$_5$)(CH$_3$)(CO)$_3$(dppm)$_2$][BF$_4$].[13] Even at −60 °C the RhOs precursor yields the butanediyl adduct [RhOs(C$_4$H$_8$)(CO)$_3$(dppm)$_2$][BF$_4$], through coupling of four methylene groups. The RhOs and IrRu compounds also differ in their tendency to lose a carbonyl ligand. Therefore, the C−C bond-formation sequences that occur in the RhOs system are accompanied by carbonyl loss, whereas the IrRu compound **4** does not lose a carbonyl upon reaction with diazomethane. The RhOs analogue of **5** (namely [RhOs(CO)$_4$(μ-CH$_2$)(dppm)$_2$][BF$_4$]) can be obtained at −80 °C; however, this product readily loses a carbonyl in the presence of excess CH_2N_2 at higher temperatures, yielding the above C_3 and C_4 products under the appropriate conditions.[13] These observations suggest that carbonyl loss is required before additional methylene groups are incorporated. If this is the case, the differences in reactivity between the RhOs and IrRu analogues can be rationalized by the process shown in Scheme 4, in which carbonyl transfer from the bridging site to the group 9 metal *precedes* carbonyl loss (dppm groups above and below the plane of the drawing are omitted). Facile carbonyl loss in related RhRe[25a] and RhOs[10] systems has been proposed to proceed via an intermediate such as **A**. In such a process the greater lability of a carbonyl from rhodium in comparison to that from iridium[36] should result in more facile CO loss from the RhOs compound than from the IrRu analogue. The structure shown for intermediate **A** has precedents in the structures described for compounds **6** and **7** (see Scheme 3).

Scheme 4

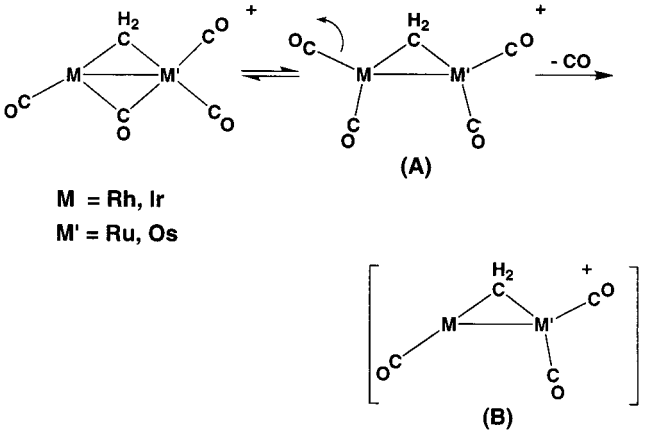

Two structural types have been observed for compounds **5**−**9** having the formulations [IrRuL(CO)$_3$(μ-CH$_2$)(dppm)$_2$][BF$_4$], as diagrammed in Scheme 3. Compounds **5**, **8**, and **9** have less symmetrical structures, in which there is only a single terminal ligand on Ir (all others being bridging), whereas compounds **6** and **7** have more symmetrical structures, possessing two terminal ligands on both Ir and Ru. We suggest that the preference for the latter structural type is strongly favored by steric effects, with the two bulkier ligands (η^2-ethylene and PMe$_3$) favoring Ir rather than the more crowded environment at Ru in the alternate structure, shown for compounds **8** and **9**. The failure of substituted olefins to form π-adducts analogous to **6** probably results from steric repulsions between these substituents and the phenyl groups of dppm. The η^1-nitrile ligands are sterically comparable to a carbonyl; therefore, similar structures are obtained with these ligands in compounds **5**, **8**, and **9**. Furthermore, assuming that the positive charge in these compounds is localized on Ru (giving a Ru(II) center), the σ-donor nitriles will be favored at this metal. The observation of the unusual nitrile-bound acrylonitrile ligand in these late-metal complexes presumably results from the need of the higher oxidation state metal for electron density and steric repulsions that inhibit π coordination of this olefin.

Carbonyl loss from **5** can be effected by reaction with trimethylamine oxide; however, the putative tricarbonyl "[IrRu(CO)$_3$(μ-CH$_2$)(dppm)$_2$][BF$_4$]", shown as structure **B** in Scheme 4, is never observed but instead readily decomposes. Since attempts to induce CO loss at lower temperature proceeded too slowly or not at all, this

(33) (a) McQueen, A. E. D.; Blake, A. J.; Stephenson, T. A.; Schröder, M.; Yellowlees, L. J. *J. Chem. Soc., Chem. Commun.* **1988**, 1533. (b) Yee, G. T.; Calabrese, J. C.; Vazques, C.; Miller, J. S. *Inorg. Chem.* **1993**, *32*, 377.

(34) (a) Rettig, M. F.; Wing, R. M. *Inorg. Chem.* **1969**, *8*, 2685. (b) Zavalii, P. Y.; Mys'kiv, M. G.; Fundomenskii, V. S. *Kristallografiya* **1984**, *29*, 60. (c) Braunswarth, H.; Huttner, G.; Zsolnai, L. *J. Organomet. Chem.* **1989**, *372*, C23. (d) Bunn, A. G.; Carroll, P. J.; Wayland, B. B. *Inorg. Chem.* **1992**, *31*, 1297. (e) Miller, J. S.; Calabrese, J. C.; McLean, R. S.; Epstein, A. J. *Adv. Mater.* **1992**, *4*, 498. (f) Cotton, F. A.; Kim, Y. *J. Am. Chem. Soc.* **1993**, *115*, 8511. (g) Cotton, F. A.; Kim, Y.; La, J. *Inorg. Chim. Acta* **1994**, *221*, 1. (h) Olmstead, M. M.; Speier, G.; Szabo, L. *J. Chem. Soc., Chem. Commun.* **1994**, 541. (i) Miller, J. S.; Vazquez, C.; Jones, N. L.; McLean, R. S.; Epstein, A. J. *J. Mater. Chem.* **1995**, *5*, 707. (j) Bohm, A.; Vazquez, C.; McLean, R. A.; Calabrese, J. C.; Kalm, S. E.; Manson, J. L.; Epstein, A. J.; Miller, J. S. *Inorg. Chem.* **1996**, *35*, 3083. (k) Vernik, I.; Stynes, D. V. *Inorg. Chem.* **1996**, *35*, 6210. (l) Sugiura, K.-I.; Mikami, S.; Tanaka, T.; Sawada, M.; Manson, J. L.; Miller, J. S.; Sakata, Y. *Chem. Lett.* **1997**, 1071. (m) Dreos, R.; Geremia, S.; Nardin, G.; Randaccio, L.; Tauzher, G.; Vuano, S. *Inorg. Chim. Acta* **1988**, *272*, 74. (n) Brandon, E. J.; Rittenberg, D. K.; Arif, A. M.; Miller, J. S. *Inorg. Chem.* **1998**, *37*, 3376.

(35) See for example: (a) Herrmann, W. A. *Adv. Organomet. Chem.* **1982**, *20*, 159 and references therein. (b) McKeer, I. R.; Cowie, M. *Inorg. Chim. Acta* **1982**, *65*, L107. (c) Azam, K. A.; Frew, A. A.; Lloyd, B. R.; Manojlović-Muir, L.; Muir, K. W.; Puddephatt, R. J. *J. Chem. Soc., Chem. Commun.* **1982**, 614. (d) Laws, W. J.; Puddephatt, R. J. *J. Chem. Soc., Chem. Commun.* **1983**, 1020.

(36) Shen, J.-K.; Tucker, D. S.; Basolo, F.; Hughes, R. P. *J. Am. Chem. Soc.* **1993**, *115*, 11312.

reaction was carried out briefly at ambient temperature, followed by cooling and subsequent substrate addition. When the reaction with excess diazomethane was carried out in this manner, the methylene-bridged ethylene adduct $[IrRu(C_2H_4)(CO)_3(\mu\text{-}CH_2)(dppm)_2][BF_4]$ (**6**) was obtained, in which two additional methylene fragments have been incorporated as the olefin. The failure of the tetracarbonyl complex **5** to react with diazomethane is in contrast to the facile reaction after removal of one carbonyl and suggests that the putative tricarbonyl complex **B** is the reactive species. It is also tempting to suggest a similar requirement in the CH_2 condensations in the RhOs system,[13] except that CO loss occurs readily in this case.

The synthesis of the acetonitrile adduct **7** was prompted by the instability of the putative tricarbonyl complex **B** and the difficulties in carrying out the transformation of **5** to **6**. It seemed that an acetonitrile ligand in such a system would be labile and that **7** might serve as a convenient source of **B** through acetonitrile loss. However, this acetonitrile ligand is not displaced in the presence of diazomethane, and **7** fails to react with this substrate. The inertness of **7** supports our earlier proposal of a Ru(II) oxidation state favoring strong binding of the σ-donor ligand.

Although the generation of the ethylene adduct **6** from the methylene-bridged precursor **5** upon reaction with diazomethane suggests the combination of the existing bridging methylene group with the newly generated methylene group, the labeling study clearly shows that this is not the case, at least for the dominant pathway. Retention of 90% of the $^{13}CH_2$ label in the bridging site indicates that the dominant pathway for methylene dimerization is occurring between unlabeled, diazomethane-generated methylene groups. In the analogous RhOs system the labeled μ-$^{13}CH_2$ group was incorporated into the C_3 or C_4 fragment, and we proposed that this was facilitated by stepwise "CH_2" insertion into the Rh−CH_2 bond of the bridging methylene group.[13] The failure of a species such as **B** to undergo an analogous methylene insertion into the Ir−(μ-CH_2) bond, although surprising, is consistent with a stronger Ir−C bond. The small amount of ^{13}C label incorporated into the ethylene ligand suggests that CH_2 insertion into either the Ir−CH_2 or the Ru−CH_2 bond of the bridging methylene group is also occurring as a secondary process. Although we have been unable to establish whether ethylene formation occurs at Ir or Ru, analogies with the RhOs chemistry suggests that activation of diazomethane and subsequent ethylene formation occurs at Ir. The blank experiment in which no ethylene is generated in the absence of compound **5** clearly establishes the involvement of an Ir/Ru complex in ethylene formation.

Conclusions

This study on the reaction of $[IrRu(CO)_4(dppm)_2][BF_4]$ with diazomethane was undertaken as a comparison with the analogous RhOs system, which was observed at temperatures above −60 °C to give rise to facile coupling of methylene units, yielding C_3 or C_4 fragments at the metals. Under similar conditions the IrRu compound yields only the methylene-bridged compound $[IrRu(CO)_3(\mu\text{-}CH_2)(\mu\text{-}CO)(dppm)_2][BF_4]$ (**5**). Although in this comparison both metals were exchanged (Ir for Rh and Ru for Os), it appears that the major difference between these two systems results from the replacement of Rh by Ir. This exchange results in two important differences that inhibit subsequent C−C bond formation. First, it inhibits CO loss, which is apparently needed before subsequent coupling of methylene groups can occur, and second, the stronger Ir−C bond involving the bridging methylene group compared to Rh−C inhibits subsequent coupling involving the bridging methylene group in the IrRu system. Coupling of methylene groups can be induced upon removal of a carbonyl from **5** in the presence of diazomethane. However, labeling studies show that the dominant pathway for ethylene formation does not involve the bridging methylene group of **5**; the ethylene ligand instead results primarily from coupling of diazomethane-generated methylene groups. The formation of ethylene from diazomethane over Fischer−Tropsch catalysts in the absence of hydrogen is well-known.[37]

Acknowledgment. We thank the Natural Sciences and Engineering Research Council of Canada (NSERC) and the University of Alberta for financial support of this research, the NSERC for funding the P4/RA/SMART 1000 CCD diffractometer, Consiglio-Nazionale delle Richerche, Rome, for salary support (to M.M.D.), and NATO for a Collaborative Research Grant (CRG 971548) with Professor P. M. Maitlis (Sheffield). M.C. acknowledges the University of Alberta for a McCalla Professorship, and thanks Professor P. M. Maitlis and Dr. M. L. Turner for helpful discussions. The help of Gerdy Aarts, who carried out the selective inversion recovery NMR experiments, and Professor R. B. Jordan, who obtained the activation parameters, is gratefully acknowledged.

Supporting Information Available: Tables of X-ray experimental details, atomic coordinates, interatomic distances and angles, anisotropic thermal parameters, and hydrogen parameters for compounds **2**, **5** and **7**. This material is available free of charge via the Internet at http://pubs.acs.org.

OM000639B

(37) Brady, R. C.; Pettit, R. *J. Am. Chem. Soc.* **1980**, *102*, 6181.